Role of individual amino acids of apolipoprotein A-I in the activation of lecithin:cholesterol acyltransferase and in HDL rearrangements

Kyung-Hyun Cho, Diane M. Durbin, and Ana Jonas[1]

Department of Biochemistry, University of Illinois at Urbana-Champaign, Urbana, IL 61801

Abstract **The central region of apolipoprotein A-I (apoA-I), spanning residues 143–165, has been implicated in lecithin:cholesterol acyltransferase (LCAT) activation and also in high density lipoprotein (HDL) structural rearrangements. To examine the role of individual amino acids in these functions, we constructed, overexpressed, and purified two additional point mutants of apoA-I (P143R and R160L) and compared them with the previously studied V156E mutant. These mutants have been reported to occur naturally and to affect HDL cholesterol levels and cholesterol esterification in plasma. The P143R and R160L mutants were effectively expressed in *Escherichia coli* as fusion proteins and were isolated in at least 95% purity. In the lipid-free state, the mutants self-associated similarly to wild-type protein. All the mutants, including V156E, were able to lyse dimyristoylphosphatidylcholine liposomes. In the lipid-bound state, the major reconstituted HDL (rHDL) of the mutants had diameters similar to wild type (96–98 Å). Circular dichroism and fluorescence methods revealed no major differences among the structures of the lipid-free or lipid-bound mutants and wild type. In contrast, the V156E mutant had exhibited significant structural, stability, and self-association differences compared with wild-type apoA-I in the lipid-free state, and formed rHDL particles with larger diameters. In this study, limited proteolytic digestion with chymotrypsin showed that the V156E mutant, in lipid-free form, has a distinct digestion pattern and surface exposure of the central region, compared with wild type and the other mutants. Reactivity of rHDL with LCAT was highest for wild type (100%), followed by P143R (39%) and R160L (0.6%). Tested for their ability to rearrange into 78-Å particles, the rHDL of the two mutants (P143R and R160L) behaved normally, compared with the rHDL of V156E, which showed no rearrangement after the 24-h incubation with low density lipoprotein (LDL). Similarly, the rHDL of V156E was resistant to rearrangement in the presence of apoA-I or apoA-II. These results indicate that structural changes are absent or modest for the P143R and R160L mutants, especially in rHDL form; that these mutants have normal conformational adaptability; and that LCAT activation is obliterated for R160L. Thus, individual amino acid changes may have markedly different structural and functional consequences in the 143–165 region of apoA-I. The R160L mutation appears to have a direct effect in LCAT activation, while the P143R mutation results in only minor structural and functional effects. Also, the processes for LCAT activation and hinge mobility appear to be distinct even if the same region of apoA-I is involved.**—Cho, K-H., D. M. Durbin, and A. Jonas. **Role of individual amino acids of apolipoprotein A-I in the activation of lecithin:cholesterol acyltransferase and in HDL rearrangements.** ***J. Lipid Res.*** **2001.** 42: **379–389.**

Supplementary key words lipoproteins • lipid binding • phospholipid • apoA-I mutants • circular dichroism • fluorescence • LCAT

Apolipoprotein A-I (apoA-I), the major protein component of high density lipoproteins (HDL), has diverse physiologic functions: lipid binding and solubilization, activation of lecithin:cholesterol acyltransferase (LCAT), modulation of HDL rearrangements during metabolism and lipid transfers, and interaction with HDL receptors on cell surfaces.

Studies of the structure-function relationships of apoA-I have been hindered by the lack of three-dimensional structures of apoA-I, especially in lipid-bound states. Nevertheless, the predicted linear organization of amphipathic helices in apoA-I (1, 2) has led to fruitful investigations of the involvement of specific sequences of apoA-I in lipid binding and LCAT activation. Thus it is now known that lipid-free apoA-I contains most of the α helices in the N-terminal half of its sequence, but that on lipid binding, the N-terminal helices rearrange and new lipid-binding helices are formed in the C-terminal half (3). In fact, most

Abbreviations: apoA-I, apolipoprotein A-I; apoA-II, apolipoprotein A-II; BS_3, bis-sulfosuccinimidyl suberate; DMPC, dimyristoylphosphatidylcholine; FC, free cholesterol; ΔG°_{D}, free energy change of denaturation; HDL, high density lipoprotein; LCAT, lecithin:cholesterol acyltransferase; LDL, low density lipoprotein; rHDL, reconstituted HDL; PAGGE, polyacrylamide gradient gel electrophoresis; POPC, 1-palmitoyl-2-oleoyl phosphatidylcholine; PVDF, polyvinylidene difluoride; WT-proapoA-I, recombinant wild-type proapoA-I; SDS-PAGE, sodium dodecyl sulfate-polyacrylamide gel electrophoresis; TBS, Tris-buffered saline; WMF, wavelength of maximum fluorescence; WT, wild type.

[1]To whom correspondence should be addressed.
e-mail: a-jonas@uiuc.edu

of the sequence of apoA-I in amphipathic helices can bind to phospholipids; however, the first and last predicted helices appear to be most important in the initial binding to lipid surfaces (4). Furthermore, the extreme C-terminal region of apoA-I is involved in interactions with HDL and cell membranes (5–7). Various deletion mutagenesis studies have also narrowed down the sequences of apoA-I that are involved in LCAT activation. There is general agreement that the sequence between residues 143–165 is most important in LCAT activation and that other regions, especially the C terminus, may have secondary roles (8–11).

While the lipid-binding and LCAT activation regions of apoA-I are fairly well demarcated, much less is known about the structural determinants of the conformational plasticity of apoA-I or its binding to receptors. Studies using specific monoclonal antibodies have suggested that a "mobile" or "hinge" region, perhaps involving a pair of amphipathic helices, exists between residues 99 and 143 of apoA-I (12, 13).

In this study we focused attention on helix 6 of apoA-I (residues 143–165), with the aim of identifying individual amino acid residues that are functionally important in LCAT activation, and to determine whether the same amino acids are involved in structural rearrangements of apoA-I. We selected three naturally occurring apoA-I mutants (P143R, V156E, and R160L) (14–17) that in clinical and in vitro investigations have suggested functional defects in apoA-I, such as decreased plasma apoA-I and HDL cholesterol levels, decreased LCAT activation, altered HDL metabolism, and in one case (V156E) coronary artery disease (16). From the molecular standpoint, these three mutations represent interesting changes in the amino acid properties of helix 6: P143R introduces a charged residue and may affect a predicted β turn or bend at the beginning of the helix; V156E replaces a hydrophobic residue in the middle of the nonpolar face of the helix with a charged amino acid; and R160L replaces a charged residue with a hydrophobic amino acid at the interface of protein and lipid.

We have already reported some of the properties of the V156E mutant, which has unique structural and functional features (18); here we extend its characterization and compare it with the two new mutant forms of apoA-I.

MATERIALS AND METHODS

Materials

Radiolabeled [4-^{14}C]cholesterol was purchased from Dupont-New England Nuclear (Boston, MA). Cholesterol, 1-palmitoyl-2-oleoyl phosphatidylcholine (POPC), sodium cholate, and TLCK-chymotrypsin were obtained from Sigma (St. Louis, MO). The Quickchange™ site-directed mutagenesis kit and pET 30a(+) expression system were purchased from Stratagene (La Jolla, CA) and Novagen (Madison, WI), respectively. The restriction enzymes and enterokinase were obtained from New England BioLabs (Beverly, MA), and Roche (Mannheim, Germany), respectively. Human apoA-I, apoA-II, and low density lipoproteins (LDL) were purified by routine methods used in our laboratory (19, 20) from blood plasma purchased from the Champaign County Blood Bank.

Vector construction

The proapoA-I mutant cDNAs were generated by polymerase chain reaction-based site-directed mutagenesis kit (Stratagene), using appropriately designed oligonucleotide primers. The following primers were produced at the Biotechnology Center of the University of Illinois at Urbana-Champaign:

P143R: 5′-CAAGAGAAGCTGAGCCGGCTGGGCGAGGAGAT GCGC-3′

R160L: 5′-GCCCATGTGGACGCGCTGTTAACGCATCTGGC CCCC-3′

Sequences of each construct were verified by appropriate endonuclease digestion and DNA sequencing, after subcloning into the expression vector, at the Biotechnology Center using an automated DNA sequencer (model 377; PE Biosystems, Foster City, CA).

Expression and purification of wild-type and mutant proteins

The expression and purification of wild-type proapoA-I (WT-proapoA-I) and mutant proapoA-I forms were carried out as described previously (18), using the pET 30a(+) expression vector and BL21 (DE3) *Escherichia coli* host cells (Novagen). After transfection of competent cells with the plasmid, a single cell colony containing the plasmid was picked and inoculated into fresh Luria-Bertani medium supplemented with kanamycin sulfate (30 μg/ml; Calbiochem, La Jolla, CA). The cells were incubated at 37°C until cell density reached 0.9–1.0 absorbance units at 600 nm. Synthesis of the histidine-tagged fusion proteins was induced by the addition of isopropyl-β-D-thiogalactopyranoside (1 mM final concentration) and the cells were incubated further, for 4 h, under the same conditions. Subsequent isolation of fusion proteins by Ni^{2+} column chromatography, removal of the histidine tag by enterokinase treatment, and delipidation of the protein-lipid complexes were carried out according to our previous protocols (18). The purified proteins were lyophilized and stored at −20°C. Prior to use, they were dissolved in 3 M guanidine hydrochloride in 0.01 M Tris buffer, pH 8.0, containing 150 mM NaCl, 0.1 mM ethylenediaminetetraacetic acid, 1 mM NaN_3 [Tris-buffered saline (TBS) buffer]; and dialyzed exhaustively against the TBS buffer.

DMPC clearance assay

Interactions of the mutant proteins with dimyristoylphosphatidylcholine (DMPC) were monitored by the method described by Pownall et al. (21) with slight modifications. Dry DMPC was dispersed in TBS (3.5 mg/ml), to form multilamellar liposomes. An aliquot of the multilamellar DMPC liposomes was added to each protein solution, to give a final concentration of protein of 0.15 mg/ml. The mass ratio of DMPC to protein was 2:1 (w/w) in 0.76 ml of total reaction volume. The measurements were initiated after addition of DMPC and monitored at 325 nm every 2 min, using a Beckman (Fullerton, CA) DU-64 spectrophotometer equipped with a thermocontrolled cuvette holder, adjusted to 24.5°C.

Preparation and characterization of POPC-rHDL particles

Discoidal reconstituted HDL (rHDL) particles were prepared by the sodium cholate dialysis method (22), using initial molar ratios of POPC/free cholesterol (FC)/apoA-I of 95:5:1. The rHDL particles contained trace amounts of [^{14}C]cholesterol when used as substrates for the LCAT reaction. The particles were used without further purification; their sizes were determined by native 8–25% polyacrylamide gradient gel electrophoresis (PAGGE), using a Pharmacia Phast system and standard

globular proteins (Pharmacia, Piscataway, NJ). Protein bands on the gels were visualized by Coomassie blue staining and were scanned with an LKB (Bromma, Sweden) Ultro Scan XL-laser densitometer. The number of protein molecules per rHDL particle, as well as the self-association behavior of the lipid-free proteins, were determined by cross-linking with bis-sulfosuccinimidyl suberate (BS_3; Pierce, Rockford, IL) as described by Staros (23). The cross-linked products were separated by sodium dodecyl sulfate-polyacrylamide gel electrophoresis (SDS-PAGE) on 8–25% gradient gels (Pharmacia) and were analyzed by densitometry.

Protein concentrations were determined by using absorbance at 280 nm and the extinction coefficients for apoA-I and proapoA-I (1.13 and 1.28 ml/mg·cm, respectively) or the Lowry protein assay as modified by Markwell et al. (24) with a bovine serum albumin standard. The phospholipid and cholesterol contents in rHDL were determined by the methods of Chen, Toribara, and Warner (25) and Heider and Boyett (26), respectively.

Circular dichroism spectroscopy

The average α-helix content of the proteins in lipid-free and lipid-bound states were measured by circular dichroism (CD) spectroscopy, using a J-720 spectropolarimeter (Jasco, Tokyo, Japan) located in the Laboratory for Fluorescence Dynamics at the University of Illinois at Urbana-Champaign. The spectra were recorded from 250 to 190 nm at 25°C in a 0.1-cm path-length quartz cuvette, using a 1.0-nm bandwidth, a speed of 50 nm/min, and 4-s response time. Four scans were accumulated and averaged. The protein samples of the lipid-free proteins were diluted to 0.07 mg/ml to avoid self-association of the apolipoproteins (3). In the rHDL lipid-bound state, the proteins were diluted to 0.1 mg/ml. The percentage of α-helical content was calculated from the molar ellipticity at 222 nm as proposed by Chen, Yang, and Martinez (27), using a mean residue weight for apoA-I of 115.3. The α-helix contents of the proteins after 1 h (lipid-free) or 72 h (lipid-bound) of incubation with increasing concentrations of guanidine hydrochloride at 4°C were used to obtain the change of free energy during unfolding (ΔG°_{D}) as described by Aune and Tanford (28) and Sparks, Lund-Katz, and Phillips (29).

Fluorescence spectroscopy

Concentrations of all samples were the same as in the CD measurements. The wavelengths of maximum fluorescence (WMF) of the tryptophan residues in WT-proapoA-I and the mutant forms were determined from uncorrected spectra obtained on a Perkin-Elmer (Norwalk, CT) LS50B spectrofluorometer using the Fluorescence (FL) WinLab software package 3.00 (Perkin-Elmer). The samples were excited at 295 nm to avoid tyrosine fluorescence, and the emission spectra were scanned from 305 to 400 nm at room temperature.

Limited proteolysis of lipid-free and lipid-bound proteins

Mild proteolysis was used to examine accessible sequences and structural differences between WT-proapoA-I and the mutant proteins (30). Each protein sample was diluted to a final concentration of 1 mg/ml in TBS buffer prior to protease treatment. The enzyme stock solutions were prepared fresh in TBS. The reactions were initiated by addition of the protease in ratios of enzyme to substrate (w/w) of 1:100, for rHDL, and of 1:200 for lipid-free apolipoprotein samples. After incubation at 25°C for the specified time intervals, aliquots were removed and were mixed with electrophoresis buffer (4% SDS) and boiled for 3 min to terminate further proteolysis. The digested samples were analyzed by SDS-PAGE, using a discontinuous Tris-tricine system (Bio-Rad, Hercules, CA), with 16.5% Tris-tricine gels (Bio-Rad Ready Gels) run in a Protean II-mini system (Bio-Rad). After electrophoresis, protein bands were transferred to polyvinylidene difluoride (PVDF) membranes for protein sequencing according to the Matsudaira procedure (31), and were visualized by Coomassie blue staining. Approximate molecular weights of the protein fragments were estimated by comparison with standard proteins (Bio-Rad low range and polypeptide standards). N-terminal protein sequencing analysis was carried out in the Protein Sciences Facility of the Biotechnology Center of the University of Illinois at Urbana-Champaign, using a Procise 494 HT system (Applied Biosystems, Foster City, CA).

LCAT assay

The LCAT reactions were carried out according to our previous procedures (32), using recombinant human LCAT (33). To initiate the reactions the recombinant LCAT (0.163 μg, 0.05 ml) was added to [^{14}C]cholesterol-POPC-rHDL substrate particles containing the various proteins and 7,500 cpm of [^{14}C]cholesterol per nanomole of FC, 4% defatted bovine serum albumin, 4 mM 2-mercaptoethanol, and TBS buffer. The POPC-rHDL substrate concentrations ranged from 1.7×10^{-7} to 1.4×10^{-6} M of apolipoprotein in a 0.5-ml reaction mixture. The samples were prepared in duplicate, and background values were determined by omitting only LCAT at each substrate concentration from the reaction tubes. The enzymatic reactions were carried out at 37°C for 30 min. Initial reaction velocities at each substrate concentration were determined by thin-layer chromatography (TLC) analysis of the lipids, and Lineweaver-Burk plots were used to obtain the apparent K_m and V_{max} values by linear regression.

Assays of conformational adaptability

To examine the conformational adaptability of the mutant proteins in POPC-rHDL particles, we monitored particle size changes on incubation of the rHDL with LDL and loss of phospholipid, as described previously (19, 34). Each POPC-rHDL preparation (100 μg of protein in 50 μl) was incubated with human LDL (120 μg of protein in 50 μl) at 37°C for up to 24 h. The structural changes were stopped at designated time intervals by the addition of native gel sample buffer and storage in 4°C prior to analysis by native 8–25% PAGGE.

To detect particle rearrangements and protein conformational adaptation on addition of lipid-free apoA-I or apoA-II to rHDL particles containing apoA-I (35, 36) or the V156E mutant, the reaction was initiated by adding apoA-I or apoA-II to POPC-rHDL (10 μg) in a 1:1 molar ratio of lipid-free apolipoproteins per HDL particle, and the mixture was incubated for 24 h at 37°C. The reaction was stopped by addition of electrophoresis sample buffer at 4°C. The reaction products were separated on 8–25% native polyacrylamide gradient gels, using the Pharmacia Phast system. Protein bands on the gel were blotted by 15 min of diffusion onto PVDF membranes (Pierce) that had been saturated with methanol to facilitate transfer. Remaining protein bands on the gel were visualized by Coomassie blue staining. The bands blotted onto the membrane were subjected to Western analysis with antibodies specific for apoA-I or apoA-II (1:7,000 dilution), following the protocol for the ImmunoPure ABC peroxidase staining kit (Pierce). Horseradish peroxidase-conjugated secondary antibodies of goat anti-rabbit and rabbit anti-goat secondary antibodies were used (1:7,000 dilution) to visualize the apoA-I and apoA-II primary antibodies, respectively. Horseradish peroxidase was detected by addition of diaminobenzidine tetrahydrochloride in 0.08% H_2O_2.

RESULTS

Purification of proteins and self-association behavior

The expression and purification of WT-proapoA-I and mutant proteins (18) gave excellent yields, ranging be-

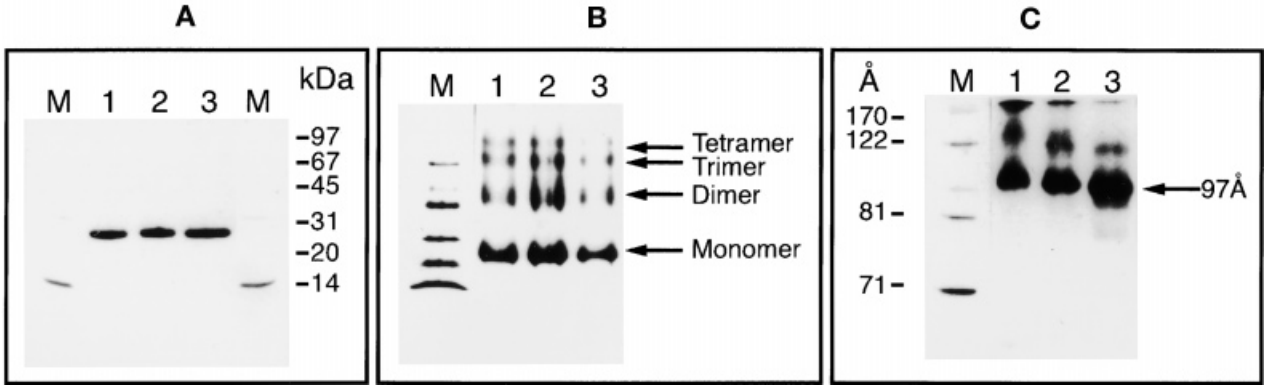

Fig. 1. Electrophoretic patterns of apolipoproteins in lipid-free and lipid-bound state. A: Purity of the recombinant mutants and WT-proapoA-I on 20% SDS-PAGE. At least 95% purity was observed by densitometric scanning. Lane M, molecular weight markers; lane 1, P143R; lane 2, R160L; lane 3, wild type. B: Self-association behavior of the apolipoproteins determined by BS_3 cross-linking. The cross-linking reaction was carried out with an aliquot of each apolipoprotein (0.7 mg/ml) for 3 h. The cross-linked products were displayed on an 8–25% SDS-polyacrylamide gradient gel. Lane M, molecular weight markers; lane 1, P143R; lane 2, R160L; lane 3, wild type. C: Electrophoretic patterns of apolipoproteins in POPC-rHDL on native 8–25% PAGGE. The rHDL were prepared by the sodium cholate dialysis method using 95:5:1 molar ratios of POPC/FC/protein. Lane M, molecular weight standards (HMW; Pharmacia); lane 1, P143R; lane 2, R160L; lane 3, wild type.

tween 20 and 37 mg of pure protein from 1 liter of cell culture. Purity was assessed by SDS-PAGE to be greater than 95% (**Fig. 1A**) for all the recombinant proteins.

In solution, at concentrations of 1.0–0.7 mg/ml, the lipid-free wild-type protein and the P143R and R160L mutants self-associated into dimers, and higher oligomers, as expected (Fig. 1B). In contrast, as shown previously (18), the V156E mutant remained mostly in the monomer form—only a small amount of dimer was observed. The same experiment performed with 0.1-mg/ml concentrations of the proteins showed that only monomeric forms were present in solution (data not shown). This was an important control as the subsequent spectroscopic experiments with the lipid-free proteins were performed at concentrations of 0.07 mg/ml to ensure that the monomer structure was investigated.

It should be noted here that studies from our laboratory (37) and others (38) have established that in vitro structural and functional properties of recombinant proapoA-I are identical to those of plasma apoA-I. Therefore, no distinctions were made between these two controls during the course of this study.

Clearance of DMPC liposomes

To investigate the surfactant-like properties of the recombinant apolipoproteins, their ability to lyse DMPC liposomes at the phase transition temperature of the phospholipid was examined. All the proteins readily solubilized the DMPC liposomes (**Fig. 2**). Under the conditions of this experiment (0.15-mg/ml initial protein concentration) the half-life ($t_{1/2}$) for liposome clearance was 16 ± 2 min for WT-proapoA-I, 17 ± 2 min for R160L, 28 ± 4 min for P143R, and 5 ± 2 min for V156E.

Preparation and characterization of POPC-rHDL particles

The rHDL particles, prepared by the sodium cholate dialysis method (22) with WT-proapoA-I and the mutant proteins at 95:5:1 molar ratios of POPC/cholesterol/protein, had diameters from 96 to 98 Å as the main products (>80% of protein stain) (see Fig. 1C). The lipid compositions of the rHDL particles are given in **Table 1**, together with the protein contents and diameters of the particles.

Spectroscopic analysis

The lipid-free and lipid-bound proteins in the rHDL particles were examined by CD and fluorescence methods to determine their secondary structure contents (percent α helix), tryptophan residue environments (WMF), and stability in the presence of guanidine hydrochloride [mid-

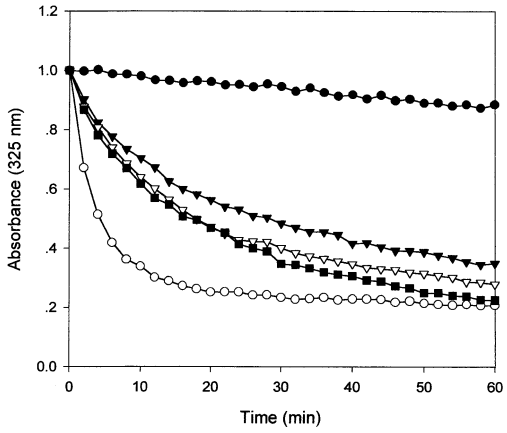

Fig. 2. Kinetics of interaction of apolipoproteins with DMPC multilamellar liposomes. The reaction was initiated by addition of 0.7 ml of apolipoproteins (0.15 mg/ml) to the multilamellar DMPC liposomes (0.06 ml, 3.5 mg/ml) in TBS, pH 8.0. The mass ratio of DMPC to protein was 2:1 (w/w) in 0.76 ml of total reaction volume. Absorbance at 325 nm was monitored at 24.5°C at 2-min intervals for up to 1 h. Buffer alone (solid circles); P143R (solid inverted triangles); R160L (open inverted triangles); wild type (solid squares); V156E (open circles).

TABLE 1. Composition and size of reconstituted HDL particles made with recombination proapoA-I (WT) and its point mutants (P143R and R160L)

rHDL	Molar Composition[a] (POPC/FC/Protein) Initial	Final	No. of Proteins/ Particle[b]	Diameter[c]
				Å
WT	95:5:1	87 ± 12:5:1	2	97
P143R	95:5:1	75 ± 17:5:1	2	97
R160L	95:5:1	83 ± 10:5:1	2	98

[a] Determined by the Lowry protein assay as modified by Markwell et al. (24), with analysis of phosphorus (25) and free cholesterol (26), in two independent reconstitution experiments.

[b] Determined by SDS-PAGE of delipidated proteins after cross-linking with BS_3.

[c] Determined by nondenaturing gradient gel (8–25%) electrophoresis, using reference globular proteins. Errors are ±2 Å.

point of denaturation ($D_{1/2}$) and ΔG°_{D}] (**Table 2**). The contents of α-helical structure were similar for WT-proapoA-I and the R160L mutant, both in the lipid-free and lipid-bound states. The P143R mutant may have had a reduced content of α helix relative to WT-proapoA-I. However, for both mutants, a marked increase in α-helical structure occurred on lipid binding in the rHDL particles.

Tryptophan WMF indicated similar, nonpolar environments of these aromatic residues for the lipid-free proteins. On lipid binding there was a consistent, small blue shift to a more nonpolar environment in all the rHDL samples.

Denaturation with guanidine hydrochloride was used to compare the stability of the different proteins. The $D_{1/2}$ and ΔG°_{D} values were similar for WT-proapoA-I and the R160L mutant, both in the lipid-free and lipid-bound states. The P143R mutant appeared to have a slightly higher stability.

Mild proteolysis

Limited proteolysis with chymotrypsin was used to compare the overall three-dimensional folding and accessibility to proteases of WT-proapoA-I and the mutant proteins, including V156E, in the lipid-free and lipid-bound states. **Figure 3** shows the chymotryptic patterns for the various samples. In the lipid-free state, the main polypeptide product had a molecular weight of 22 kDa for the wild-type, P143R, and R160L proteins, and corresponded to cleavage at Tyr-192, as previously reported for plasma apoA-I (30). In contrast to this result, the V156E mutant in the lipid-free state exhibited a markedly different proteolysis pattern: the main products of the enzymatic digestion were 12- and 13-kDa fragments, corresponding to cleavage at residues Leu-122 and Leu-200, indicating a major structural change in this mutant with respect to the wild-type protein.

In the lipid-bound state the reaction kinetics of the enzymatic digestion were much slower, but after 12 h all the rHDL samples produced the same major proteolytic fragment of 22 kDa because of cleavage at Tyr-192. This indicates that all the proteins in rHDL form were quite resistant to proteolysis and had comparable three-dimensional structures.

TABLE 2. α-Helix content and denaturation parameters of lipid-free and lipid-bound recombinant proapoA-I (WT) and mutants (P143R and R160L)

Apolipoprotein	α-Helix Content[a]	WMF[b]	$D_{1/2}$[c]	ΔG°_{D}[d]
	%	*nm*	*M, GndHCl*	*kcal/mol apoA-I*
WT	58	337	1.2	2.4
P143R	45	337	1.6	2.9
R160L	59	338	1.3	2.6
WT-POPC-rHDL	76	335	3.3	2.5
P143R-POPC-rHDL	61	334	3.6	2.7
R160L-POPC-rHDL	74	334	3.4	2.4

[a] Determined from molar ellipticity at 222 nm. Errors are ±7%.

[b] The errors of measurement were about ±2 nm for the WMF of Trp residues.

[c] Guanidine hydrochloride (GndHCl) concentration for 50% denaturation of the protein.

[d] Standard free energy change of denaturation. For the rHDL particles the ΔG°_{D} is an apparent value because the denaturation is not a reversible process at all concentrations of GndHCl. Errors were on the order of ±0.3 kcal/mol.

LCAT activation

After establishing that the structures and stabilities of the mutants were similar to WT-proapoA-I in the lipid-bound state, functional assays were performed. The previously determined larger size of V156E-rHDL (18) was not a major concern in the functional comparisons, because we had previously shown that larger rHDL particles containing apoA-I and POPC or egg phosphatidylcholine (egg-PC), with α-helix content similar to that of the 96-Å rHDL species, had similar reactivities with LCAT (39). **Figure 4** depicts the initial reaction velocity as a function of protein concentration in rHDL substrate particles, and **Table 3** summarizes the apparent kinetic constants. The reactivity (apparent V_{max}/K_m) of P143R was reduced to about 40% of WT-proapoA-I, and the reactivity of the V156E and R160L mutant rHDL was minimal (less than 1% of wild type). Both, changes in apparent V_{max} and apparent K_m were responsible for the reduced reactivity of these mutant rHDL.

Conformational adaptability

The ability of the WT-proapoA-I and the mutants to rearrange their structures in response to changes in lipid content of the rHDL was examined by nondenaturing gradient gels as the rHDL particles were exposed to LDL. **Figure 5** shows the time course of the particle rearrangements for wild-type, P143R, V156E, and R160L-rHDL particles. Although the slow rearrangement kinetics may be somewhat different, after 24 h little of the original 96- to 98-Å particles of wild type, P143R, and R160L remained, and there was massive conversion to 87-Å intermediates and/or 78-Å products (19). In contrast, confirming our previous report (18), the V156E-rHDL did not rearrange during the 24-h incubation.

To confirm further that the V156E-rHDL had indeed an impaired ability for conformational adaptation, a different experiment was performed with this mutant. Ad-

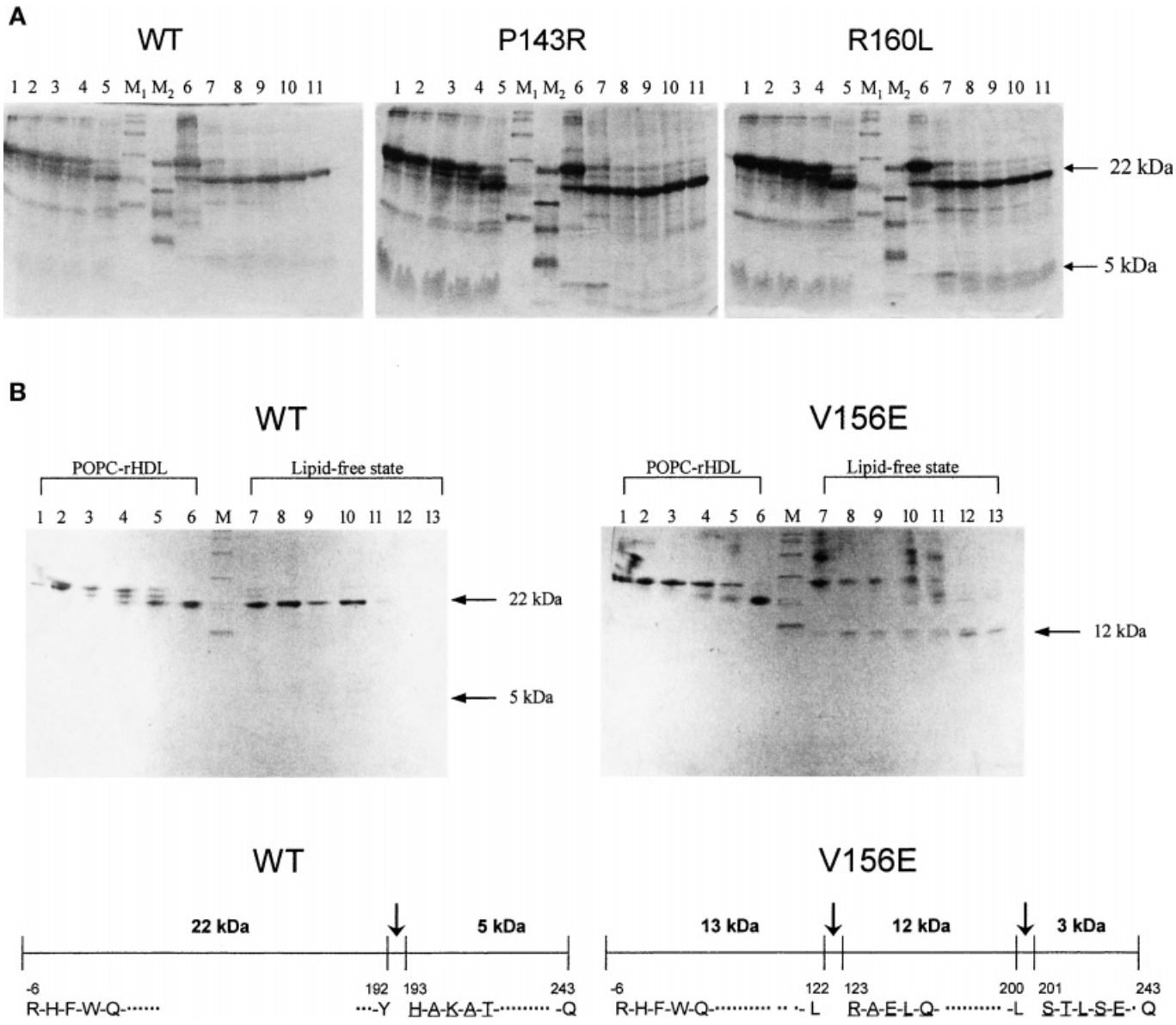

Fig. 3. Chymotrypsin digestion patterns of apolipoproteins in lipid-bound and lipid-free state. TLCK-chymotrypsin was added in 1:100 and 1:200 ratios (w/w) to the proteins in POPC-rHDL complexes and in the lipid-free state, respectively. The reaction mixtures were incubated at 25°C; at designated times, aliquots were removed and the reaction was terminated by addition of 4% SDS and boiling for 3 min. The samples were stored in −20°C until electrophoresis. The digestion products were separated by 16.5% SDS-PAGE, using the Tris-tricine buffer system (Bio-Rad). A: Lanes 1 through 5 display digestion patterns of proteins in POPC-rHDL complexes. Lanes 1, 2, 3, 4, and 5 correspond, respectively, to 0, 10, 30, 120, and 720 min of incubation time. Lane M_1, Bio-Rad low range standards (14, 20, 31, 45, 67, and 97 kDa). Lane M_2, Bio-Rad polypeptide molecular weight standards (3.5, 6.5, 14, 17, and 27 kDa). Lanes 6 through 11 show the digestion patterns of lipid-free apolipoproteins. Lanes 6, 7, 8, 9, 10, and 11 correspond, respectively, to 0, 1, 10, 20, 40, and 80 min of incubation time. In all reactions, the major product was a fragment of about 22 kDa. B: Lanes 1 through 6 show the digestion patterns of the proteins in POPC-rHDL complexes. Lanes 1, 2, 3, 4, 5, and 6 correspond, respectively, to 0, 5, 10, 30, 120, and 720 min of incubation time. Lane M, Bio-Rad low range standards (14, 20, 31, 45, 67, and 97 kDa). Lanes 7 through 13 show the digestion patterns of lipid-free proteins. Lanes 7, 8, 9, 10, 11, 12, and 13 correspond, respectively, to 0.5, 1, 5, 10, 20, 40, and 80 min of incubation time. In the lipid-free state, the major products were about 22- and 5-kDa fragments in wild-type samples. The 5-kDa fragment was shown to begin at His-193 as determined by amino acid sequencing. In the lipid-free V156E samples 12-, 13-, and 3-kDa fragments predominated. N-terminal sequencing revealed that proteolysis had occurred at the carboxyl side of Leu-122 and Leu-200. The underlined amino acids were identified by N-terminal sequencing.

dition of lipid-free apoA-I or apoA-II to rHDL particles, containing apoA-I and POPC, was previously shown to result in initial rapid binding of the apolipoproteins followed by a slow rearrangement of the apoA-I structure and particle sizes (35, 36). However, addition of apolipoproteins to the V156E-rHDL particles did not lead to structural changes (see **Fig. 6**), although binding of the apolipoproteins did occur as demonstrated by Western blotting and fluorescence polarization experiments (data not shown).

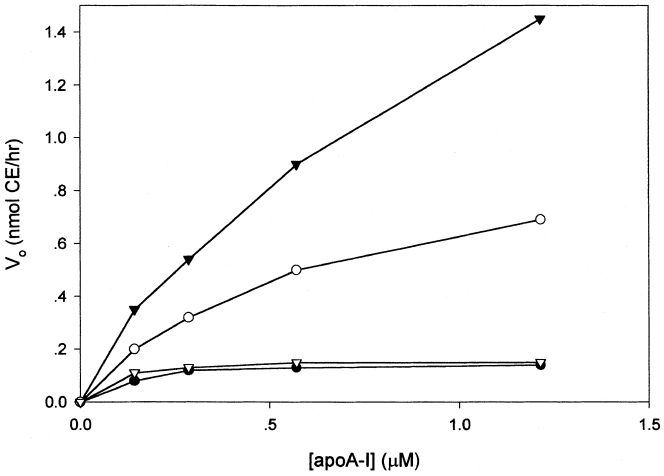

Fig. 4. Kinetics of the LCAT reaction with POPC-rHDL substrates. The rHDL were prepared with molar ratios of 95:5:1:150 (POPC/FC/protein/sodium cholate). The symbols correspond to initial velocities as a function of apolipoprotein concentrations for wild-type (solid inverted triangles), P143R (open circles), and R160L (open inverted triangles) rHDL complexes. V156E-rHDL (solid circles) was used as a negative control.

DISCUSSION

Lipid-free proteins

Although lipid-poor or lipid-free apoA-I is only a minor component found in circulation, compared with lipid-bound apoA-I, its metabolic roles in HDL remodeling (35, 36) and in lipid uptake from cells (40) are essential in the reverse cholesterol transport process. Thus the issues of apoA-I behavior and structure in solution, and interactions with lipids, are of major interest in lipoprotein metabolism and function.

In this study, various methods were used to examine the structure of two natural mutants of apoA-I (P143R and R160L) in solution, including CD and fluorescence spectroscopic methods, limited proteolytic digestion, and self-association behavior. Also, the previously described mutant V156E (18) was characterized further and compared with the new mutants. In globular, water-soluble proteins such nonconservative mutations would be expected to perturb structure, especially if the amino acid substitutions were in the hydrophobic core, or in turns of the polypeptide chain. However, in contrast to globular proteins, apoA-I in solution has a low free energy of denaturation (3, 37, 41) and is thought to exist in a molten-globule state without a defined three-dimensional structure (42). Therefore, the effects of these mutations on apoA-I structure could not be easily predicted. We found, in fact, that the structural properties of the R160L mutant in solution were indistinguishable from those of WT-proapoA-I. In most respects, the P143R mutant also resembled WT-proapoA-I, with the difference that the α-helix content of the P143R appeared lower. However, in contrast to the P143R and R160L mutants, the V156E mutant had altered structural properties as indicated by its decreased interaction with guanidine hydrochloride (higher midpoint of denaturation), a marginally higher stability, and a small red shift in tryptophan fluorescence wavelength maximum (18). The ability of the V156E mutant to self-associate was impaired (18), and its proteolytic digestion pattern was altered, indicating major changes in the surface exposure of amino acid residues in the middle region of the sequence. Apparently Val-156 is critically important in maintaining the normal solution conformation of apoA-I.

TABLE 3. Reaction of rHDL particles with LCAT[a]

Apolipoprotein POPC-rHDL	Apparent[b] V_{max}	Apparent K_m	Apparent V_{max}/App. K_m
	nmol CE/h	*μM*	*nmol CE/h · M* × 10^{-6}
WT-POPC-rHDL	2.6 ± 0.3	0.8 ± 0.1	3.3 ± 0.2
P143R-POPC-rHDL	1.5 ± 0.3	1.2 ± 0.2	1.3 ± 0.2
R160L-POPC-rHDL	0.2 ± 0.03	9.0 ± 1.4	0.02

[a] Values are expressed as the mean ± error from two independent LCAT assays that used duplicate samples.

[b] The apparent kinetic parameters were determined by linear regression analysis, using a Lineweaver-Burk plot of the reciprocals of the initial reaction velocity versus the substrate concentration (protein concentration in rHDL).

Lipid-bound proteins

A simple and popular test of apolipoprotein interactions with phospholipids is their ability to solubilize DMPC liposomes (21). In this assay we monitored the complex process of apolipoprotein binding to the lipid surface, penetration of the bilayer (usually at the phase transition temperature of the phospholipid), and breakdown of the liposomes into discoidal micelles as a single process by the decrease in light scattering with time. All the apolipoprotein forms in this study were able to lyse DMPC liposomes, but surprisingly, the V156E mutant had more rapid kinetics than wild type and the other mutants. This may be because V156E is mostly monomeric at 0.15 mg/ml, while the other protein solutions may also contain some oligomeric forms. Alternatively, the introduction of a glutamate in the sequence may lead to salt bridge formation with an adjacent basic residue, thus decreasing hydration and local polarity. This would promote interaction with the DMPC bilayer. In the case of the P143R mutant, the decreased rate of DMPC lysis may be attributed either to the decrease in α-helical structure or to excess charge in this mutant.

In spite of these differences in the lysis of DMPC liposomes, all mutants formed rHDL particles with POPC at 95:5:1 POPC/cholesterol/protein (molar ratios), by the sodium cholate dialysis method. The resulting rHDL particles were similar in composition, size, and protein structure for wild-type, P143R, and R160L mutants. The V156E mutant formed larger particles, enriched in phospholipid, as previously reported (18). Nevertheless V156E-rHDL was similar in apolipoprotein folding to wild-type apoA-I in rHDL form, as revealed by proteolytic digestion and the spectroscopic results.

Taking into account the overall similarity of the apolipoprotein structures in the rHDL states, we proceeded

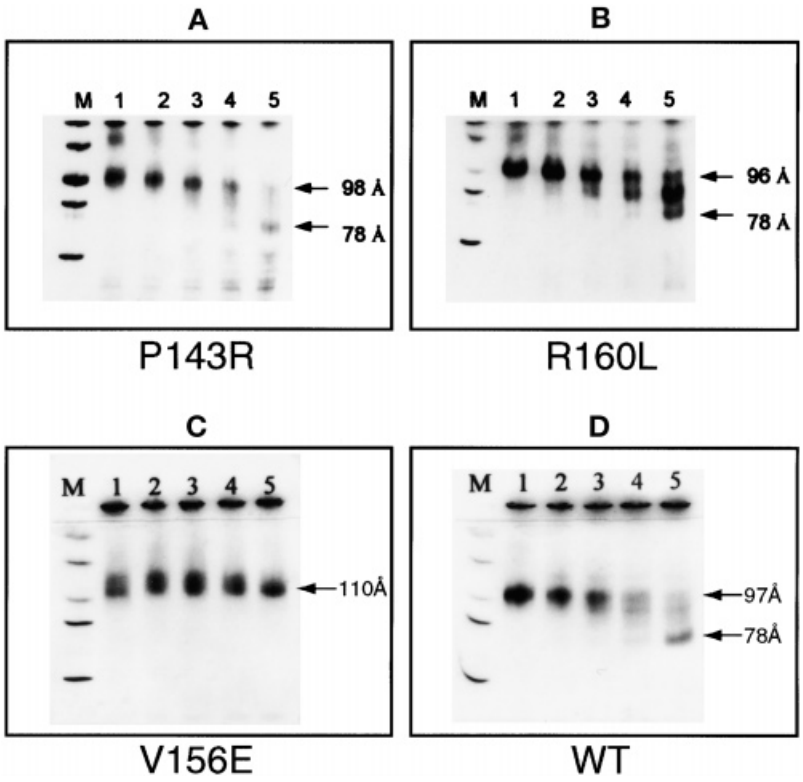

Fig. 5. Rearrangement patterns of rHDL particles in the presence of LDL. Approximately equal protein amounts in rHDL (100 μg) and LDL (120 μg) were incubated at 37°C for up to 24 h. Aliquots of the incubation mixture were removed at timed intervals and stored at 4°C in gel-loading buffer without SDS. The samples were separated on 8–25% native gels, and protein bands were visualized by Coomassie blue staining. The rearrangement patterns of (A) P143R-rHDL, (B) R160L-rHDL, (C) V156E-rHDL (used as a negative control) (18), and (D) wild-type rHDL are shown. In each panel lane M has high molecular weight markers, and lanes 1, 2, 3, 4, and 5 correspond, respectively, to 0, 4, 8, 12, and 24 h of incubation. These experiments were reproduced at least twice.

with functional analyses of LCAT activation and conformational adaptability of the mutants.

LCAT activation

In this study we focused on the role of individual amino acids in helix 6 of apoA-I in LCAT activation. The results indicated that the P143R mutation decreased LCAT activation by about 60%. This effect may be attributed to a local structural change at the beginning of this key helix, whose deletion (10), sequence reversal (9), or substitution (43) is known to decrease dramatically the reactivity of LCAT with substrate particles containing the modified apoA-I. In the original description of this natural mutation, found by isoelectrofocusing screening of a large population for apoA-I mutants, Utermann et al. (14) did not report on the clinical status of the heterozygous donor, but showed that in vitro, this apoA-I was less effective in activating LCAT by about 40–60%. This result is similar to our current observation with the recombinant P143R mutant.

In the case of the V156E and R160L mutants we observed a dramatic inhibition of the LCAT reaction. Their rHDL had less than 1% of wild-type rHDL reactivity (apparent V_{max}/apparent K_m) with LCAT. This result is comparable to apoA-II rHDL behavior, which is characteristic of an apolipoprotein that is not an activator of LCAT (35, 36). In these cases the inhibition is due to an increased

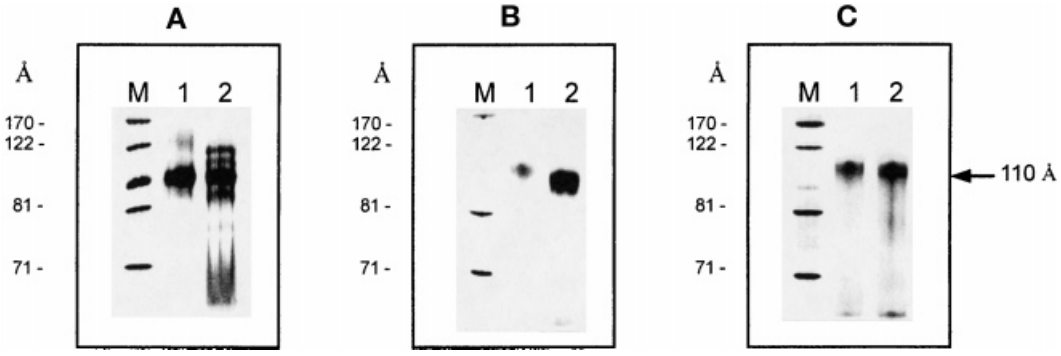

Fig. 6. Effect of apolipoprotein addition on rHDL particle rearrangement. A: The effect of lipid-free apoA-I added to control apoA-I rHDL in a 1:1 molar ratio (added apoA-I/rHDL) and incubated at 37°C for 24 h. Lane M, standard proteins; lane 1, rHDL before incubation; lane 2, rHDL after incubation. Proteins were separated and displayed on 8–25% native gels. B: Lane 1, V156E-rHDL before incubation with apoA-I; lane 2, V156E-rHDL after incubation with apoA-I for 24 h at 37°C. C: Lane 1, V156E-rHDL before incubation with apoA-II; lane 2, V156E-rHDL after incubation with apoA-II (1:1, apoA-II/rHDL molar ratio) for 24 h at 37°C.

apparent K_m and a decreased apparent V_{max}. By analogy with apoA-II rHDL reaction with LCAT, the increased K_m may be due to an increase in dissociation rate constant, which is reflected in a lower binding affinity for LCAT (44), and a decreased V_{max}, reflecting a decreased catalytic rate constant due to impaired activation.

For the R160L mutant, which did not have a significant effect on apoA-I structure, the effect on LCAT activation and affinity was likely due to a direct role of Arg-160 in the process. Because the LCAT reaction is sensitive to salt concentration and anion effects (45) and the effective charge on apoA-I (46), it is likely that the positively charged Arg-160 group is intimately involved in LCAT activation. The inhibition of LCAT activation by the V156E mutation is quantitatively similar to that of R160L. Indeed, in the putative helix 6, both these residues (Val-156 and Arg-160) are separated by only one turn of the helix, and are close in space to each other. Thus a direct effect of Val-156 on LCAT activation could be invoked. However, the larger size of the V156E-rHDL does suggest some structural differences for this lipid-bound mutant compared with wild type; therefore, structural effects cannot be discounted in this case.

Both these mutations (V156E and R160L) were shown to affect LCAT activity in vivo and in vitro in the original reports on these natural mutants (16, 17). For the V156E homozygous mutant, LCAT mass and cholesterol esterification were reduced to about 50% of normal (16). The residual cholesterol esterification presumably occurred on LDL and HDL containing apoE and apoC-I, as observed in other apoA-I deficiencies; and the decreased mass of LCAT was connected to the markedly reduced apoA-I and HDL-C concentrations in this patient. Indeed, the reduced apoA-I and HDL-C were probably the consequence of an impaired maturation of apoA-I-containing particles and their increased catabolism. Interestingly, the V156E homozygous patient had coronary artery disease (16).

The first report by Leren et al. (15) on heterozygous carriers of the R160L mutation indicated 50–70% lower levels of HDL-C and apoA-I, and an impaired ability to form large HDL particles containing both apoA-I and apoA-II. A subsequent in vitro study (17) showed only a modest decrease (29%) in LCAT activation when using DPPC-rHDL particles containing the purified R160L mutant. This apparent discrepancy with our results may be due to the use of DPPC-rHDL substrates, which are about 10-fold less reactive with LCAT than POPC-rHDL particles. Nevertheless, the decreased HDL-C and apoA-I levels in the patients may be similarly attributed to the impaired maturation of HDL containing the R160L mutant.

Conformational adaptability

It is well known that apoA-I can undergo major structural changes not only in the conversion from the lipid-free to a lipid-bound state, but also in diverse lipid-bound forms, as HDL lipids are metabolized or transported between lipoproteins and membranes, or the HDL are modified by apolipoprotein binding. The structural basis for such conformational flexibility probably resides in "mobile" or "hinge" regions of apoA-I (12, 13, 19). Perhaps the simplest model is based on the reduction in size of reconstituted discoidal HDL when phospholipids are lost to acceptors such as LDL (19, 34). The reduction in the rHDL diameter is not gradual; rather, it occurs in steps that suggest the removal of one or two helices of apoA-I from contact with lipid (34). Furthermore, these conformational changes in apoA-I are accompanied by major functional effects such as a marked inhibition of LCAT activation (34) or reduced binding to scavenger receptor class B type I receptors (D. van Der Westhuyzen and D. M. Durbin, unpublished results). Similarly, addition of lipid-free apolipoproteins to discoidal rHDL leads to particle rearrangements and inhibition of LCAT activation (36), as well as structural changes of the apoA-I originally present on the rHDL particle (35).

The apoA-I regions involved in structural rearrangements have been demarcated by specific monoclonal antibody binding experiments, between residues 99 and 143 of the sequence (12, 13). In addition, the vicinity of Lys-107 was implicated in another study, which showed that the deletion of this residue inhibits rHDL rearrangement (47). The fact that LCAT activation is drastically inhibited in rHDL particles that have rearranged from 96- to 78-Å diameters (34) suggests that helix 6 and perhaps adjacent helices are involved. Furthermore, limited proteolytic cleavage of apoA-I on rHDL particles with bound apoA-II indicates structural changes near residues 116–123 (35).

In this study we examined the individual amino acids of helix 6 that have dramatic effects on LCAT activation, for their effects on apoA-I conformational adaptability, using the assays of rHDL rearrangement in the presence of LDL, or apoA-I and apoA-II binding to rHDL.

The P143R and R160L mutants could not be distinguished from WT-proapoA-I in their conformational adaptation to form smaller rHDL; however, as already described (18), V156E-rHDL were defective in the formation of 78-Å particles when the original rHDL were exposed to LDL. In the new assay of apolipoprotein binding followed by rHDL rearrangement, the V156E mutant was also defective. Thus it appears that the V156E mutation has local structural effects that prevent apoA-I conformational changes, perhaps by increasing helix-helix interactions or sterically interfering with the conformational change. In contrast, the P143R and R160L point mutations did not prevent apoA-I conformational changes, even when they were inhibitory to the LCAT reaction. Therefore, it can be inferred that LCAT activation and conformational adaptation are distinct processes even if they may involve overlapping apoA-I regions.

From this study, and the preceding one (18), we conclude that three different point mutations in helix 6 of apoA-I have varied structural and functional effects. While the P143R mutant has modest structural and functional effects, the R160L mutant appears to have minimal structural effects but causes a major inhibition of the LCAT reaction, probably because of a direct role of Arg-160 in LCAT activation. Finally, the V156E mutant has structural and functional effects that render the apoA-I

incapable of activating LCAT and undergoing conformational adaptation.

This work was supported by National Institutes of Health grants HL-16059 and HL-29939.

Manuscript received 31 July 2000 and in revised form 25 October 2000.

REFERENCES

1. Boguski, M. S., M. Freeman, N. A. Elshourbagy, J. M. Taylor, and J. I. Gordon. 1986. On computer-assisted analysis of biological sequences: proline punctuation, consensus sequences, and apolipoprotein repeats. *J. Lipid Res.* **27:** 1011–1034.
2. Segrest, J. P., M. K. Jones, H. De Loof, C. G. Brouillette, Y. V. Venkatachalapathi, and G. M. Anantharamaiah. 1992. The amphipathic helix in the exchangeable apolipoproteins: a review of secondary structure and function. *J. Lipid Res.* **33:** 141–166.
3. Davidson, W. S., T. Hazlett, W. W. Mantulin, and A. Jonas. 1996. The role of apolipoprotein A-I domains in lipid binding. *Proc. Natl. Acad. Sci. USA.* **93:** 13605–13610.
4. Palgunachari, M. N., V. K. Mishra, S. Lund-Katz, M. C. Phillips, S. O. Adeyeye, S. Alluri, G. M. Anantharamaiah, and J. P. Segrest. 1996. Only the two end helixes of eight tandem amphipathic helical domains of human apoA-I have significant lipid affinity. *Arterioscler. Thromb. Vasc. Biol.* **16:** 328–338.
5. Sviridov, D., L. E. Pyle, and N. Fidge. 1996. Efflux of cellular cholesterol and phospholipid to apolipoprotein A-I mutants. *J. Biol. Chem.* **271:** 33277–33283.
6. Holvoet, P., Z. Zhao, E. Deridder, A. Dhoest, and D. Collen. 1996. Effects of deletion of the carboxyl-terminal domain of apoA-I or of its substitution with helices of apoA-II on *in vitro* and *in vivo* lipoprotein association. *J. Biol. Chem.* **271:** 19395–19401.
7. Laccotripe, M., S. C. Makrides, A. Jonas, and V. I. Zannis. 1997. The carboxyl-terminal hydrophobic residues of apolipoprotein A-I affect its rate of phospholipid binding and its association with high density lipoprotein. *J. Biol. Chem.* **272:** 17511–17522.
8. Minnich, A., X. Collet, A. Roghani, C. Cladaras, R. L. Hamilton, C. J. Fielding, and V. I. Zannis. 1992. Site-directed mutagenesis and structure-function analysis of the human apolipoprotein A-I. *J. Biol. Chem.* **267:** 16553–16560.
9. Sorci-Thomas, M. G., L. Curtiss, J. S. Parks, M. J. Thomas, M. W. Kearns, and M. Landrum. 1998. The hydrophobic face orientation of apolipoprotein A-I amphipathic helix domain 143–164 regulates lecithin:cholesterol acyltransferase activation. *J. Biol. Chem.* **273:** 11776–11782.
10. Sorci-Thomas, M. G., M. Thomas, L. Curtiss, and M. Landrum. 2000. Single repeat deletion in apoA-I blocks cholesterol esterification and results in rapid catabolism of Δ6 and wild-type apoA-I in transgenic mice. *J. Biol. Chem.* **275:** 12156–12163.
11. Holvoet, P., B. De Geest, S. Van Linthout, M. Lox, S. Danloy, K. Raes, and D. Collen. 2000. The Arg123-Tyr166 central domain of human apoA-I is critical for lecithin:cholesterol acyltransferase-induced hyperalphalipoproteinemia and HDL remodelling in transgenic mice. *Arterioscler. Thromb. Vasc. Biol.* **20:** 459–466.
12. Marcel, Y. L., P. R. Provost, H. Koa, E. Raffai, N. Vu Dac, J-C. Fruchart, and E. Rassart. 1991. The epitopes of apolipoprotein A-I define distinct structural domains including a mobile middle region. *J. Biol. Chem.* **266:** 3644–3653.
13. Bergeron, J., P. G. Frank, S. Damon, Q-H. Meng, G. Castro, and Y. L. Marcel. 1995. Apolipoprotein A-I conformation in reconstituted discoidal lipoproteins varying in phospholipid and cholesterol content. *J. Biol. Chem.* **270:** 27429–27438.
14. Utermann, G., J. Haas, A. Steinmetz, R. Paetzold, S. C. Rall, Jr., K. H. Weisgraber, and R. W. Mahley. 1984. Apolipoprotein $A\text{-}I_{Giessen}$ ($Pro^{143}\rightarrow Arg$). *Eur J. Biochem.* **144:** 325–331.
15. Leren, T. P., K. S. Bakken, U. Daum, L. Ose, K. Berg, G. Assmann, and A. von Eckardstein. 1997. Heterozygosity for apolipoprotein $A\text{-}I\ (R160L)_{Oslo}$ is associated with low levels of high density lipoprotein cholesterol and HDL-subclass LpA-I/A-II but normal levels of HDL-subclass LpA-I. *J. Lipid Res.* **38:** 121–131.
16. Huang, W., J. Sasaki, A. Matsunaga, H. Nanimatsu, K. Moriyama, H. Han, M. Kugi, T. Koga, K. Yamaguchi, and K. Arakawa. 1998. A novel homozygous missense mutation in the apoA-I gene with apoA-I deficiency. *Arterioscler. Thromb. Vasc. Biol.* **18:** 389–396.
17. Daum, U., T. P. Leren, C. Langer, A. Chirazi, P. Cullen, P. H. Pritchard, G. Assmann, and A. von Eckardstein. 1999. Multiple dysfunctions of two apolipoprotein A-I variants, $apoA\text{-}I\ (R160L)_{Oslo}$ and apoA-I(P165R), that are associated with hypoalphalipoproteinemia in heterozygous carriers. *J. Lipid Res.* **40:** 486–494.
18. Cho, K. H., and A. Jonas. 2000. A key point mutation (V156E) affects the structure and functions of human apolipoprotein A-I. *J. Biol. Chem.* **275:** 26821–26827.
19. Jonas, A., K. E. Kédzy, M. I. Williams, and K-A. Rye. 1988. Lipid transfers between reconstituted high density lipoprotein complexes and low density lipoproteins: effects of plasma protein factors. *J. Lipid Res.* **29:** 1239–1357.
20. Leroy, A., and A. Jonas. 1994. Native-like structure and self-association behavior of apolipoprotein A-I in water/n-propanol. *Biochim. Biophys. Acta.* **1212:** 285–294.
21. Pownall, H. J., J. B. Massey, S. K. Kusserow, and A. M. Gotto, Jr. 1978. Kinetics of lipid-protein interactions: interaction of apolipoprotein A-I from human plasma high density lipoproteins with phosphatidylcholines. *Biochemistry.* **17:** 1183–1188.
22. Matz, C. E., and A. Jonas. 1982. Micellar complexes of human apolipoprotein A-I with phosphatidylcholines and cholesterol prepared from cholate-lipid dispersions. *J. Biol. Chem.* **257:** 4535–4540.
23. Staros, J. V. 1982. *N*-Hydroxysulfosuccinimide active esters:bis(*N*-hydroxysulfo-succinimide) esters of two dicarboxylic acids are hydrophilic, membrane-impermeant, protein cross-linkers. *Biochemistry.* **21:** 3950–3955.
24. Markwell, M. A. K., S. M. Haas, L. L. Bieber, and N. E. Tolbert. 1978. A modification of the Lowry procedure to simplify protein determination in membrane and lipoprotein samples. *Anal. Biochem.* **87:** 206–210.
25. Chen, P. S., Jr., T. Y. Toribara, and H. Warner. 1956. Microdetermination of phosphorus. *Anal. Chem.* **28:** 1756–1758.
26. Heider, J. G., and R. L. Boyett. 1978. The picomole determination of free and total cholesterol in cells in culture. *J. Lipid Res.* **19:** 514–518.
27. Chen, Y-H., J. T. Yang, and H. M. Martinez. 1972. Determination of the secondary structures of proteins by circular dichroism and optical rotatory dispersion. *Biochemistry.* **11:** 4120–4131.
28. Aune, K. C., and C. Tanford. 1969. Thermodynamics of the denaturation of lysozyme by guanidine hydrochloride. II. Dependence on denaturant concentration at 25 degrees. *Biochemistry.* **8:** 4586–4590.
29. Sparks, D. L., S. Lund-Katz, and M. C. Phillips. 1992. The charge and structural stability of apolipoprotein A-I in discoidal and spherical recombinant high density lipoprotein particles. *J. Biol. Chem.* **267:** 25839–25847.
30. Ji, Y., and A. Jonas. 1995. Properties of an N-terminal proteolytic fragment of apolipoprotein A-I in solution and in reconstituted high density lipoproteins. *J. Biol. Chem.* **270:** 11290–11297.
31. Matsudaira, P. 1987. Sequence from picomole quantities of proteins electroblotted onto polyvinylidene difluoride membranes. *J. Biol. Chem.* **262:** 10035–10038.
32. Matz, C. E., and A. Jonas. 1982. Reaction of human lecithin cholesterol acyltransferase with synthetic micellar complexes of apolipoprotein A-I, phosphatidylcholine, and cholesterol. *J. Biol. Chem.* **257:** 4541–4546.
33. Jin, L., Y. P. Lee, and A. Jonas. 1997. Biochemical and biophysical characterization of human recombinant lecithin:cholesterol acyltransferase. *J. Lipid Res.* **38:** 1085–1093.
34. Jonas, A., K. E. Kédzy, and J. H. Wald. 1989. Defined apolipoprotein A-I conformations in reconstituted high density lipoprotein discs. *J. Biol. Chem.* **264:** 4818–4824.
35. Durbin, D. M., and A. Jonas. 1997. The effect of apolipoprotein A-II on the structure and function of apolipoprotein A-I in a homogeneous reconstituted high density lipoprotein particle. *J. Biol. Chem.* **272:** 31333–31339.
36. Durbin, D. M., and A. Jonas. 1999. Lipid-free apolipoproteins A-I and A-II promote remodelling of reconstituted high density lipoproteins and alter their reactivity with lecithin:cholesterol acyltransferase. *J. Lipid Res.* **40:** 2293–2302.
37. McGuire, K. A., W. S. Davidson, and A. Jonas. 1996. High yield overexpression and characterization of human recombinant proapolipoprotein A-I. *J. Lipid Res.* **37:** 1519–1528.

38. Sorci-Thomas, M. G., J. S. Parks, M. W. Kearns, G. N. Pate, C. Zhang, and M. J. Thomas. 1996. High level secretion of wild-type and mutant forms of human proapoA-I using baculovirus-mediated Sf-9 cell expression. *J. Lipid Res.* **37:** 673–683.
39. Jonas, A., and H. T. McHugh. 1984. Reaction of lecithin:cholesterol acyltransferase with micellar substrates. Effect of particle sizes. *Biochim. Biophys. Acta.* **794:** 361–372.
40. Forte, T. M., R. Gothgoldstein, R. W. Nordhausen, and M. R. McCall. 1993. Apolipoprotein A-I cell membrane interaction. Extracellular assembly of heterogeneous nascent HDL particles. *J. Lipid Res.* **34:** 317–324.
41. Tall, A. R., D. M. Small, G. G. Shipley, and R. S. Lees. 1975. Apoprotein stability and lipid-protein interactions in human plasma high density lipoproteins. *Proc. Natl. Acad. Sci. USA.* **72:** 4940–4942.
42. Gursky, O., and D. Atkinson. 1996. Thermal unfolding of human high-density apolipoprotein A-I: implications for a lipid-free molten globular state. *Proc. Natl. Acad. Sci. USA.* **93:** 2991–2995.
43. Sorci-Thomas, M. G., L. Curtiss, J. S. Parks, M. J. Thomas, and M. W. Kearns. 1997. Alteration in apolipoprotein A-I 22-mer repeat order results in a decrease in lecithin:cholesterol acyltransferase reactivity. *J Biol. Chem.* **272:** 7278–7284.
44. Jin, L., J-J. Shieh, E. Grabbe, S. Adimoolam, D. Durbin, and A. Jonas. 1999. Surface plasmon resonance biosensor studies of human wild-type and mutant lecithin cholesterol acyltransferase interactions with lipoproteins. *Biochemistry.* **38:** 15659–15665.
45. Jonas, A., J. L. Daehler, and E. R. Wilson. 1986. Anion effects on the reaction of lecithin-cholesterol acyltransferase with discoidal complexes of phosphatidylcholines—apolipoprotein A-I-cholesterol. *Biochim. Biophys. Acta.* **876:** 474–485.
46. Sparks, D. L., P. G. Frank, S. Braschi, T. A-M. Neville, and Y. L. Marcel. 1999. Effect of apolipoprotein A-I lipidation on the formation and function of pre-β and α-migrating LpA-I particles. *Biochemistry.* **38:** 1727–1735.
47. Jonas, A., A. von Eckardstein, K. E. Kédzy, A. Steinmetz, and G. Assmann. 1991. Structural and functional properties of reconstituted high density lipoprotein discs prepared with six apolipoprotein A-I variants. *J. Lipid Res.* **32:** 97–106.